# DESIGN AND EXPERIMENTAL VALIDATION OF A MINIATURE REAL-TIME POLYMERASE CHAIN REACTION DEVICE USING DISPOSABLE MICROFLUIDIC CHIPS

By

Dustin L. House

Thesis

Submitted to the Faculty of the

Graduate School of Vanderbilt University

in partial fulfillment of the requirements

for the degree of

MASTER OF SCIENCE

In

Mechanical Engineering

December, 2008

Nashville, TN

Approved:

Dr. Haoxiang Luo

Dr. D. Greg Walker

Dr. Dongqing Li

ACKNOWLEDGEMENTS

Let me first begin by thanking my advisor, Dr. Dongqing Li. His passion for science and technology served as motivation for all of us. I am thankful for the experience to have worked within a laboratory where scientific breakthroughs were a regular occurrence. I wholeheartedly believe that the work done by him and those around him will revolutionize the field of handheld medical devices.

Secondly, I must acknowledge Dr. Chan Hee Chon. His vast knowledge in the field of mechanical engineering served as a bottomless source of answers and ideas. Not to be forgotten are fellow graduate students within my laboratory for providing assistance during challenging moments.

For their time and assistance within this project, I also would like to express gratitude to Dr. Buddy Creech, Dr. Erik Skaar, and Brian McKenna. Their insight within the ever-important study of methicillin-resistant *Staphylococcus aureus* (MRSA) will help countless people around the world. For her ability to clearly explain the more complex areas of biochemistry to an engineer, I thank Dr. Susan Opalenik.

I must also extend my appreciation towards the School of Engineering at Vanderbilt University and the H. Fort Flowers Foundation for their financial support. Without the support of either, none of this would have been possible.

Finally, I express sincere gratitude to my parents, Kendall and Vickie House, and my sister, Brandy House, for there endless love and support through all my endeavors.

TABLE OF CONTENTS

LIST OF FIGURES

Page

Figure

# CHAPTER I

## INTRODUCTION

Since its inception in the mid-80s, the polymerase chain reaction (PCR) has become a catalyst that drives biological and medical research. The simplicity of its technique has allowed for its integration within fields such as drug discovery, molecular archaeology, forensics, microbial detection, and most notably the diagnosis of both genetic and infectious diseases. Following its introduction to the field of microfluidics [1], scientists and engineers have worked to exploit the advantages of this tandem including the ability to reduce reagent consumption, cost, and reaction time and in particular, improve portability and automation. With the integration of a miniature fluorescent detection module [2-4], these lab-on-a-chip (LOC) systems near the realization of a fully-integrated portable real-time PCR system useful for point-of-care testing of highly infectious agents, such as methicillin-resistant *Staphylococcus aureus* (MRSA). Vast research has been performed in the field of micro-PCR using purified genomic DNA. Still, clinical usefulness of this technology has not yet been realized as sample preparation steps taken prior to PCR are time consuming at a macro-scale and introduce complex problems on the micro-scale. This research pushes the limits of the required sample preparation steps in an effort to introduce an on-site diagnostic device for MRSA.

## Thesis Overview

The goal of the work detailed within this thesis was to design and experimentally validate, as a proof of concept, a miniature real-time polymerase chain reaction system for use as a diagnostic device. A miniature thermal cycler and micro-well bioreactor were designed and continuously redesigned to improve simplicity, efficacy and repeatability. Positive and negative control samples were tested alike at varying concentrations under various preparation procedures. Results were monitored through a DNA-specific fluorescent reporter and fluorescent microscope followed by verification through gel electrophoresis. The organization of this thesis is as follows:

- *Chapter 1* describes the motivation behind the thesis topic and provides a thorough literature review of previous research within the field.
- *Chapter 2* introduces the theory governing the polymerase chain reaction with more recent techniques of quantification.
- *Chapter 3* follows the evolution of the miniature thermal cycler and microfluidic chip as their designs are continuously improved in an effort to create a more efficient system.
- *Chapter 4* details the experimental methods used in fabrication and to set up the reaction and collect fluorescent data.
- *Chapter 5* presents the experimental results and their respective validation.
- *Chapter 6* highlights the major conclusions and describes future work required on the system.

## Literature Review

Micro-PCR systems are typically classified into two categories based on the design of their microfluidic chip: stationary well-based chips and continuous flow-through chips. Stationary well-based chips function in a manner similar to a conventional PCR system, but much smaller. The sample is loaded into a stationary micro-reaction chamber (a well), sealed, and then cycled through the required temperatures by means of a miniature thermal cycler commonly in the form of an external heat source such a thin film heating element [5-7] or a Peltier thermoelectric component [8-10]. Other types of heat sources utilize the photothermal effect to reduce the dependency of thermal contact between the microfluidic chip and its heat source. Forms of light utilized in this technique include an infrared light [11-13], a halogen lamp to reduce power consumption and cost [14] and a diode laser to focus the light and thus improve efficiency [15,16]. Another technique investigated for heating has been the use of an external fluid to improve heat transfer; specifically, the use of hot air [17]. Continuous flow-through chips function contrastingly. Generally, the sample is loaded into a well and then moved through a network of microfluidic channels passing through the required temperature zones [18-20]. A novel approach to the flow-through design utilizes convection-driven flow to move the fluid through temperature zones [21,22]. One hindrance for flow-through systems is the unalterable number of cycles dependent upon chip design. Obeid et al. has proposed a manner of avoiding this through the addition of outgoing channels located after specific increments of cycles to collect the product [23]. Hu et al. also successfully verified Joule heating potential to simplify chip design in this flow-through approach to PCR

microfluidics while offering more control over assay parameters [24].

Both forms of PCR microfluidic chips have advantages and disadvantages. It is typically accepted that flow-through chips are able to reduce reaction times by their inherently more efficient heat transfer. Stationary chips, however, are simple in design and offer universality with respect to assay parameters such as temperature and holding time. What makes stationary well-based chips desirable is the ability to easily integrate fluorescent detection components for real-time data collection and the adaptability for high-throughput screening. When comparing disadvantages of each, consistency across wells with respect to temperature and fluorescence is typically mentioned when describing stationary high throughput micro-well-based chips (and their macro counterparts). Without careful design, inconsistency of these parameters can lead to differences in amplification and sensitivity, ultimately leading to a lack of repeatability. In the same manner, flow-through micro-PCR chips are typically viewed as more complex due to their structure. The efficacy of flow-through chips is more sensitive to their design and manufacturing. Consequently, this form of chip can be more expensive. With the belief that simplicity is optimal for the progression of lab-on-a-chip devices used in point-of-care diagnoses, this paper investigates the detection of MRSA based on different degrees of sample preparation through the use of simple, inexpensive, disposable microfluidic chips. In stark contrast to silicon or glass chips manufactured through typical photolithography, metal deposition, etching and oxidation processes, the chips used in this work are formed using standard soft lithography of polydimethylsiloxane (PDMS). The simplicity of this process allows

for rapid production of disposable chips, thus eliminating contaminations associated with cleaning and reusing PCR chips. These chips are utilized with a small thermal cycler consisting of a stage used to apply pressure to the well, a thin resistance heater beneath the chip and a small cooling fan. To obtain real-time fluorescent data, the thermal cycler was placed on the stage of a fluorescent microscope. This system is proposed as an inexpensive method for running a real-time micro-PCR reaction for MRSA.

In recent years, methicillin-resistant *Staphylococcus aureus* has emerged as a danger outside of its traditional setting of health care institutions. This epidemic of community-associated MRSA has led to a dramatic increase in skin and soft-tissue infections, osteoarticular infections, and bacteremia in the United States [25-28]. Treatment of CA-MRSA becomes complex due to the limited choice of antibiotics and the frequent need for invasive surgery. It was estimated through 2004-5 that nearly 100,000 individuals endured invasive community-associated MRSA infections. 20,000 of which resulted in fatality [29]. Although much research is being done in the area of treatment, another problem arises in the time that is required to accurately diagnose infections. Through the processes of culture, isolation and identification, at least 48 hours will have passed (from the time of culture). This can lead to ineffective antibiotics that do little to prevent the spread of the infection. Developments in real-time PCR have reduced the time to detection but still cannot offer bedside diagnostics from raw samples such as the drainage from a wound. Thus, a portable, rapid diagnostic system would have significant clinical application.

# CHAPTER II

## POLYMERASE CHAIN REACTION

To understand the impact of the work detailed in this study it is necessary that the reader have a fundamental understanding of the polymerase chain reaction. In 1983, Kary Mullis discovered that a temperature-controlled reaction incorporating a mixture of nucleotides, primers, and DNA polymerase can create billions of copies of a target gene from only a single strand of DNA. The applications of such a simple DNA amplification process are numerous and for his discovery, he was awarded the 1993 Nobel prize.

### The Process

The polymerase chain reaction, to put it simply, is a manner of replicating (amplifying) specific, or entire sequences of deoxyribonucleic acid (DNA). The primary components involved in a typical reaction include free nucleotides, oligonucleotide primers, and a DNA polymerase. Primers define the region of the DNA strand to be copied, nucleotides serve as building blocks for the new strands of DNA and the polymerase acts as a cayalyst for DNA synthesis. The process is controlled by altering the temperature of the sample. Many polymerase chain reactions begin with an extended denaturation. During this stage, the sample is held at the denaturing temperature of 54 ºC. At this temperature, the hydrogen bonds between corresponding base pairs within the DNA duplex break down and the strands separate,

or denature, as shown in Figure 1(a,b). A longer initial denaturing process is used to ensure the original template (at times an entire genome) is thoroughly separated before thermal cycling. This step is followed by an annealing process in which the sample is held at a temperature (commonly ranging from 45 to 65 ºC) that is dependent upon the design of the sequence-specific oligonucleotide primers. At this temperature, the primers hybridize, or anneal, to the template DNA at their respective locations. These primers are synthetically-produced short DNA strands (oligonucleotides) that align to the template DNA based on Watson and Crick base pairing rules. When annealed to the template, they flank the specific gene (DNA segment) that is to be replicated in the reaction (see Figure 1(c)). The final step in the cycle is an extension phase during which the thermostable polymerase forms the polymerized DNA molecule. The temperature of this process is optimized for the polymerase and is commonly around 72 ºC. Deoxynucleotides (dNTPs, free nucleotides) are then utilized by the enzyme to reconstruct the desired DNA duplex starting from the primer. This process is visualized in Figure 1(d-f). Once the new molecule is fully synthesized, the reaction temperature is raised to the denaturing temperature to repeat the process using the newly formed molecules. Figure 1(g,h) shows the resulting products formed during the second and third cycles. Notice that, theoretically, a fully synthesized target gene is not formed until after the third cycle is complete. By its nature, the DNA polymerase will continue constructing a complimentary strand from base-pairing rules until it physically or chemically can go no further. Thus, until a complimentary strand of specified length is formed after the second cycle, the polymerase can not stop itself during the replicating process.

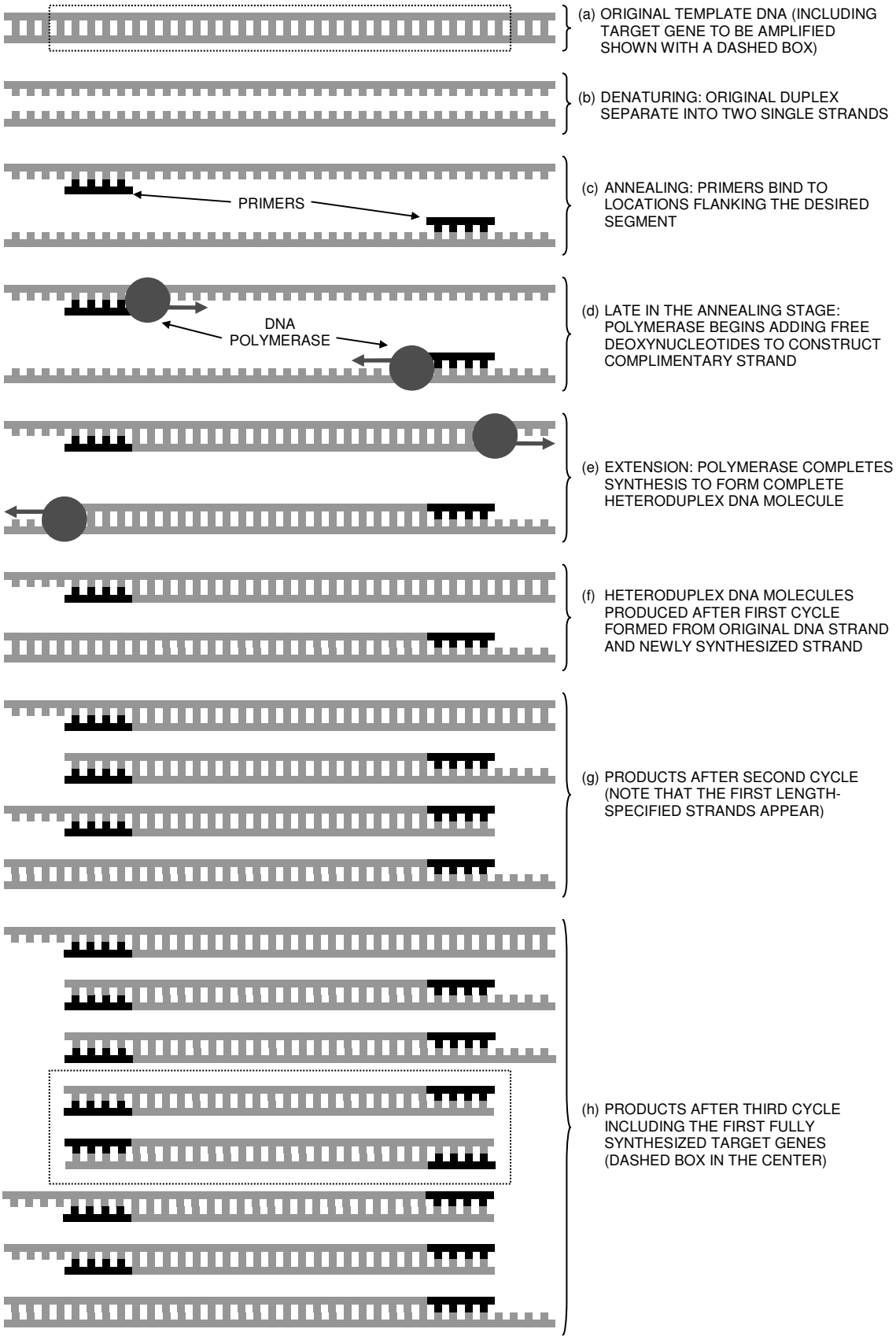


**Figure 1**. Diagram showing each of the steps throughout the polymerase chain reaction.

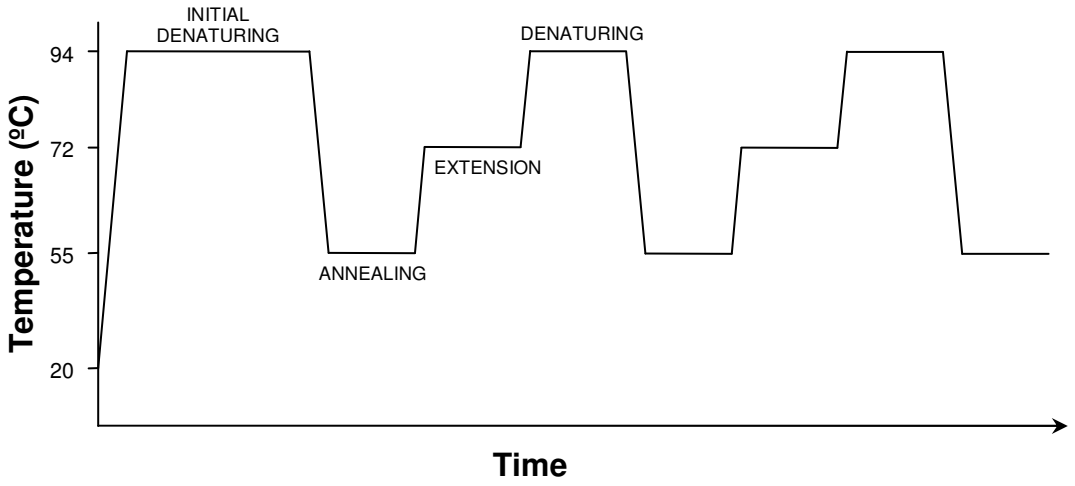


**Figure 2**. A generalized theoretical temperature curve during the initial cycles of a polymerase chain reaction.

As was previously implied, the thermal steps are cycled. This process is depicted in Figure 2 with theoretical temperature curves. By its nature, the reaction is a doubling process which yields an exponential increase in the number of amplicons (newly formed DNA strands) produced in subsequent cycles. Thus, with just a small amount of DNA, 11.2 pg in this study, it is possible to produce enough DNA molecules to run common biological analyses. Theoretically, one could generate over 1,000,000 product strands from just one initial DNA strand through 20 cycles, however, contamination, inadequate optimization, primer-to-primer annealing and various other complications reduce the efficiency of a reaction. If one were able to plot the exact number of amplicon produced as a function of time over a period of 40 cycles, the resulting trend should resemble a sigmoidal curve such as the one seen in Figure 3. During the initial cycles of the polymerase chain reaction, there are far more unused primers in the mixture than template DNA strands. These primers continue searching for their respective complimentary sequence strands and tend to bind to

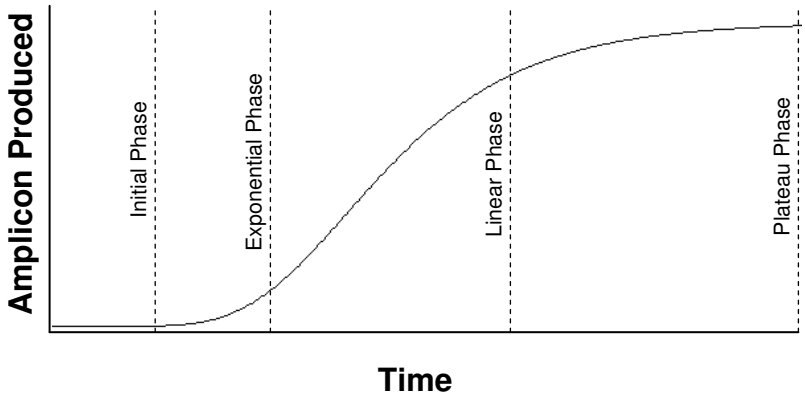


**Figure 3**. A theoretical plot visualizing the kinetic effect of reagents on the amplicon production over time

locations that are only partially correct. The efficiency of the reaction increases as thermal cycling continues due to the increasing ratio of template strands to primers. This phase is typically characterized as the exponential phase as the doubling of target strands becomes more apparent. The exponential phase tends to become linear as the reaction efficiency peaks (the slope is indicative of this efficiency). As the kinetics change, the reaction eventually reaches a plateau. It is at this point when the limiting reagent, typically the DNA polymerase, prevents further amplicon production. Also, the ratio of template strands to primers becomes so large that product strands tend to bind to themselves when searching for primers. Thermal cycling should halt before the reaction reaches this stage.

## Post-Processing

Upon completion of the polymerase chain reaction, an analysis is required to ensure that the process was completed successfully. With regards to diagnostics, this step serves to provide evidence as to whether a particular gene was found present in

the sample. One of the most common techniques employed in laboratories is gel electrophoresis. This process is capable detecting the size of DNA molecules present within a sample. In preparation for gel electrophoresis, an agarose gel slab is formed and submerged in an aqueous solution. After completing PCR, a portion of each sample is loaded into individual wells located within the end of the gel slab. Prior to loading, these samples are typically mixed with glycerol and a marker dye. Glycerol raises the density of the injected sample to assist in loading and the dye provides visualization of the molecules under ultraviolet light. Each well within the slab has its own lane through which the DNA migrates. One of the lanes is loaded with a ladder containing markers that provide reference sizes for the samples. Electrodes are attached to both ends of the loaded gel and a voltage is applied. The induced electric field drives the negatively charged DNA molecules toward the anode. This migration rate is heavily dependent upon the molecule's size, or its strand length. An inverse relationship between molecular size and migration rate allows the smaller molecules to migrate farther through their respective lanes within the gel when compared to the larger molecules. Frictional forces generated between the migrating molecules and the polymeric structure of the gel drive this electrophoretic separation. After a period of time, the voltage is removed and the gel is viewed under ultraviolet light. This allows for the visualization of bands that form from marked DNA molecules within the loaded samples. These bands are then compared to marker bands found within the reference ladder that correspond to known molecule sizes to determine the size of DNA molecules within the loaded samples. Figure 4 depicts a common setup for a slab prepared for gel electrophoresis with theoretical bands. Figure 5 is an example of

the resulting image of a slab when viewed under ultraviolet light.

## Real-time PCR

A quantitatively more powerful approach to the polymerase chain reaction is an alternate method appropriately titled real-time polymerase chain reaction. This form of the reaction allows one to track the amplicon production throughout the process using optical detection. Only a single reagent separates the composition of a sample used in real-time polymerase chain reaction from that of conventional PCR: a.fluorescent reporter. This study utilizes an oligonucleotide probe

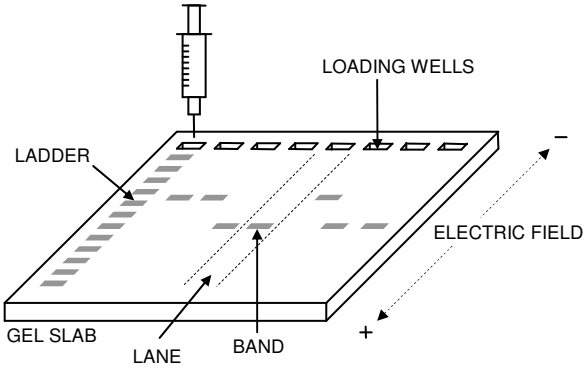


**Figure 4**. An example of a gel electrophoresis setup with hypothetical bands formed from migrating DNA molecules

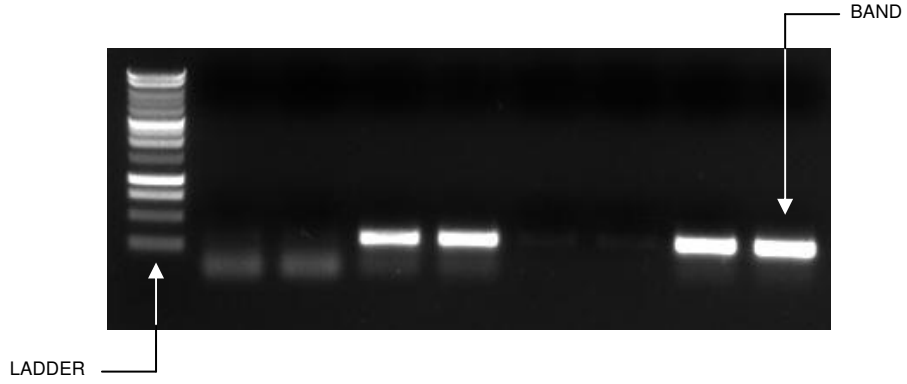


**Figure 5**. Resulting picture of an agarose gel slab after gel electrophoresis when viewed under an ultraviolet light

specifically designed to compliment the target gene. One end of this molecular probe holds a reporter dye while the other end holds a quencher dye. During the annealing stages of thermal cycling, this probe binds itself to a target region of the DNA to be copied. As the DNA polymerase begins synthesis during the extension phase, it frees the reporter dye from the oligonucleotide probe. Prior to this release, the fluorophore (reporter dye) and quencher dye endure fluorescence resonance energy transfer (FRET) in which (due to their close proximity) the fluorescence emitted by the reporter dye is absorbed by the quencher dye. Once cleaved, the fluorescence emitted by the reporter dye is no longer absorbed by the quencher dye. This release yields an overall increase in measurable fluorescence. As cycling proceeds, more reporter dyes are free to emit light due to the production of more DNA molecules. The fluorescence monitored during each stage is proportional to the number of fluorophores released from their oligonucleotides, and therefore the amount of DNA molecules currently within the sample.

When the recorded fluorescence is plotted versus cycles completed throughout the duration of an assay, the resulting curve should resemble that of the curve seen in Figure 3. During the initial cycles, the fluorescence emitted by the fluorophores is not strong enough to distinguish itself from the background fluorescence so the curve is normalized with this baseline flouorescence value. Once the assay reaches the exponential phase, measured fluorescence rises above the baseline fluorescence and, over time, takes on the form of the theoretical sigmoidal curve. The primary advantage offered with this variation of the polymerase chain reaction is the ability to

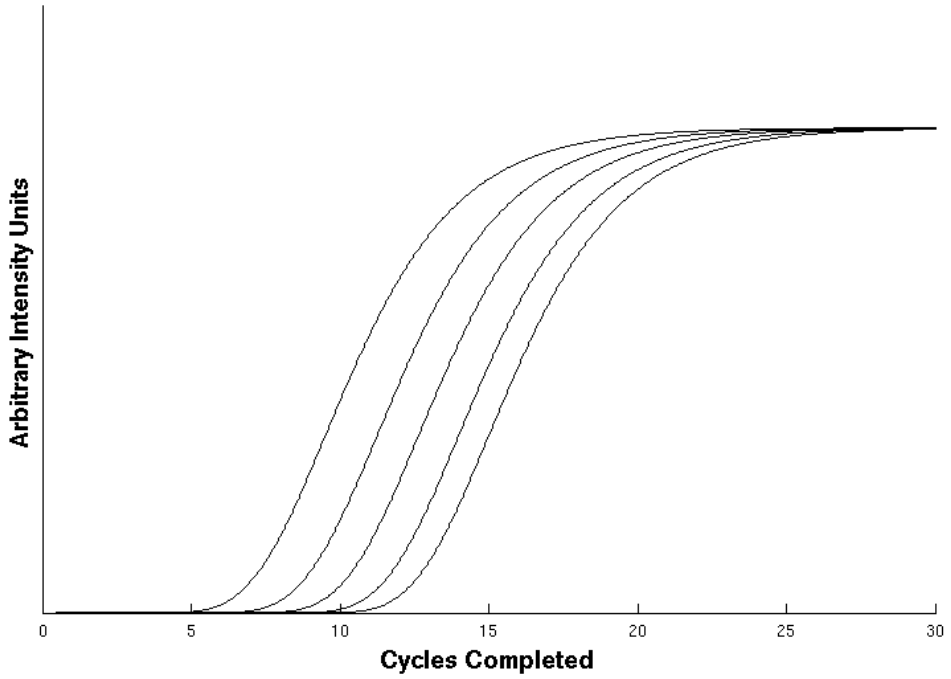


**Figure 6**. Example of a series of fluorescent intensity curves generated from real-time PCR performed on samples of varying initial template DNA concentration.

extract the initial template concentration from previously calibrated data. This ability is grounded in the fact that a reaction conducted on a sample with a higher concentration of template DNA is detectable at an earlier cycle. The initial cycle at which the fluorescent intensity curve is significantly higher than the baseline fluorescence is known as the threshold cycle, $C_T$. If a series of reactions are performed on samples of known template concentration, it is possible to create a standard curve representing the threshold cycle of a reaction versus the log of the initial concentration. Figure 6 is an example of what a fluorescence plot would look like if the data from each reaction were overlaid in this process. Notice each of the curves has a different threshold cycle dependent upon their respective initial template DNA concentration. In order to more accurately determine the threshold cycle, a

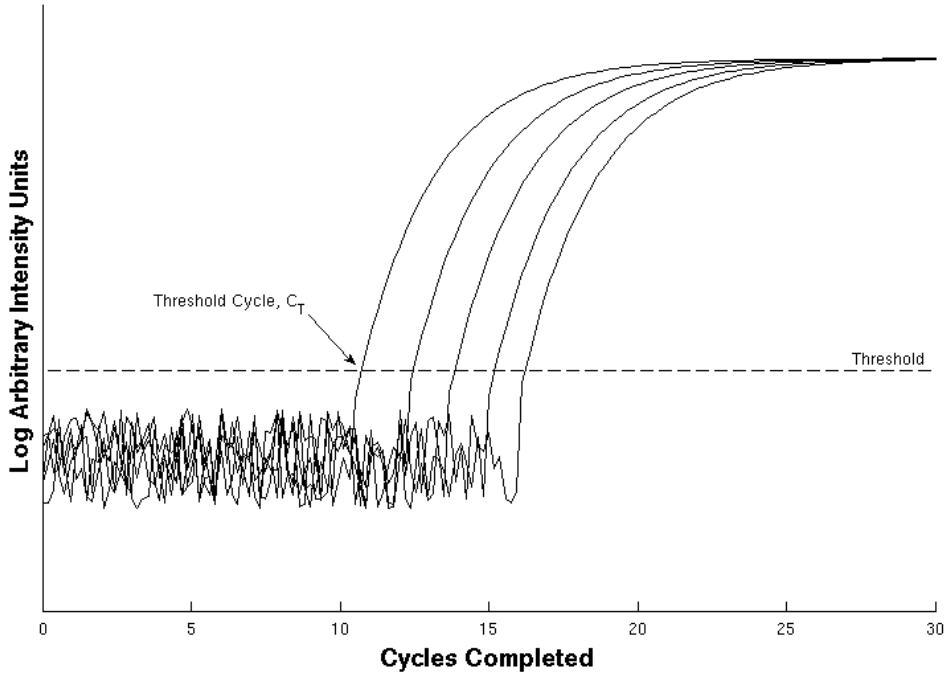


**Figure 7**. The logarithmic fluorescent intensity plot created to determine the threshold fluorescence and corresponding threshold cycle numbers for each series of data.

logarithmic fluorescent plot (such as the one seen in Figure 7) is typically employed. This plot provides a clearer representation of the log-linear phase and it is within this phase that the threshold cycle number should be chosen to provide the most accurate results. As was previously mentioned, it is from the collected threshold cycle data that the standard curve is generated. An example of a standard curve is depicited in Figure 8. It is from this plot that one can extrapolate the initial concentration of DNA from a sample by experimentally determining the threshold cycle.

More information can be gathered from the standard curve if the theory is expanded. Mathematically, the concentration of the template DNA during the exponential phase of the reaction can be described with the following expression,

$$X_n = X_o E^n \qquad \text{Eq. 1}$$

where $X_n$ is the template concentration at the $n^{th}$ cycle, $X_o$ is the initial template concentration and $E$ is efficiency of the reaction. An ideal reaction would have an efficiency of 2, representing a doubling in the concentration after each cycle. If Equation 1 is arranged to represent a standard curve, it would take on the following form,

$$n = -\frac{1}{\log E}\log X_o + \frac{\log X_n}{\log E} \qquad \text{Eq. 2}$$

where $X_n$ represents the concentration of template at the $n^{th}$ cycle. In this form the reaction efficiency can be easily calculated from the slope of the linear fit of the standard curve.

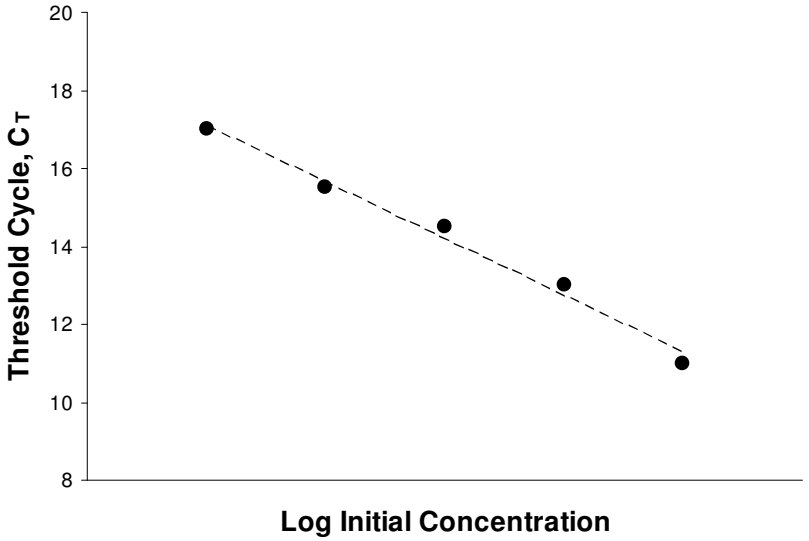


**Figure 8**. Example of a standard curve generated from the threshold cycle numbers experimentally obtained from samples of known concentrations

# CHAPTER III

# DESIGN OF SYSTEM AND FABRICATION

## Heater and Chip Functionality

The work performed in the area of micro-PCR within our lab was divided into two areas. While one researcher, Dr. Chan Hee Chon, focused on the electrical and optical detection systems, my efforts were directed toward the improvement of the design of the microfluidic chip and thermal cycler. All work was centered on the development of a portable real-time PCR system. Due to emphasis on simplicity within this study, a stationary, well-based chip was used to perform the biological assays. As described previously, this style of microfluidic chip allows for the easy adjustment of reaction parameters and is conducive to the integration of a fluorescent detection system to collect real-time data. The primary piece of the chip consisted of a thin square prism of PDMS that had been patterned on one side by soft lithography. The pattern design used in previous works within this laboratory consisted of four wells, each found within its own raised cylindrical surface seen in Figure 9. Between these short cylindrical platforms were shallow draining channels crossing in the center of the chip and continuing to the edge of the flat sides of the chip. For structural support, and to serve as the bottom of the well, a glass coverslip was bonded to the unpatterned side of the PDMS. Prior to use, the wells of this chip were slightly overfilled with the sample. A thin, circular PDMS lid then covered each well individually and was pressed against the chip for adequate sealing.

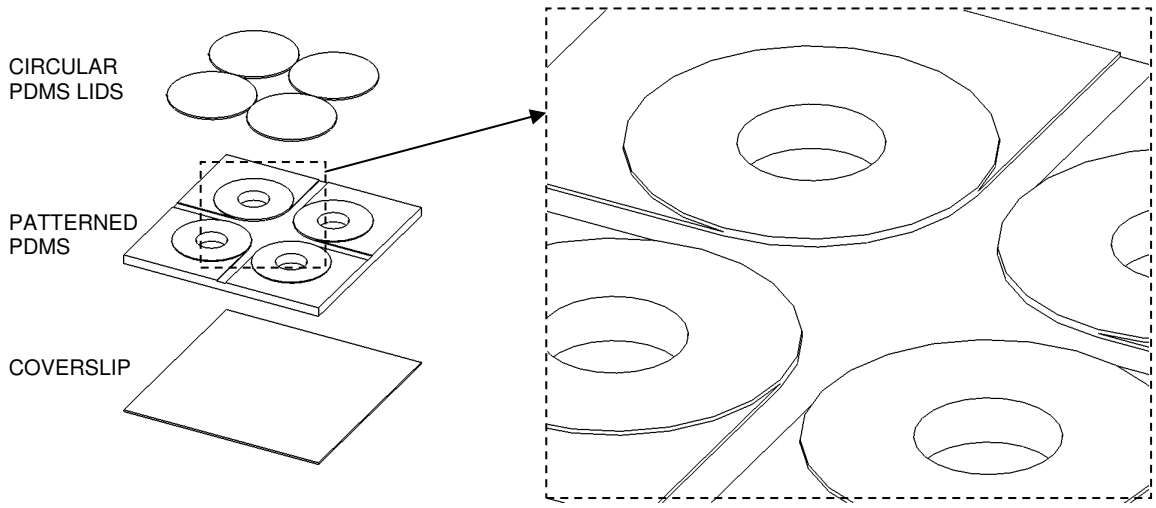


**Figure 9**. An early design of the microfluidic chip used in micro-PCR assays.

This setup allowed for overflow of the sample to flow into the draining channels in order to prevent intermixing.

Once the chips were assembled, they were loaded into the thermal cycler. In this study, the thermal cycler utilized a thin resistive heating element and a blower-style fan to quickly cycle through temperatures. The chip was placed on an adjustable stage that could be lowered and raised toward a ceiling made of a transparent material. A drawing of the first generation thermal cycler is shown in Figure 10. The objective of the thermal cycler was to hold the chip under pressure and to heat or cool the chip when required. Pressure was applied for two reasons. It increased heat transfer between the heating element and the reaction chamber by reducing contact resistance. It also served to prevent the formation of bubbles within the reaction chamber and ultimately sample evaporation. Another requirement of the thermal cycler was the ability to easily load and

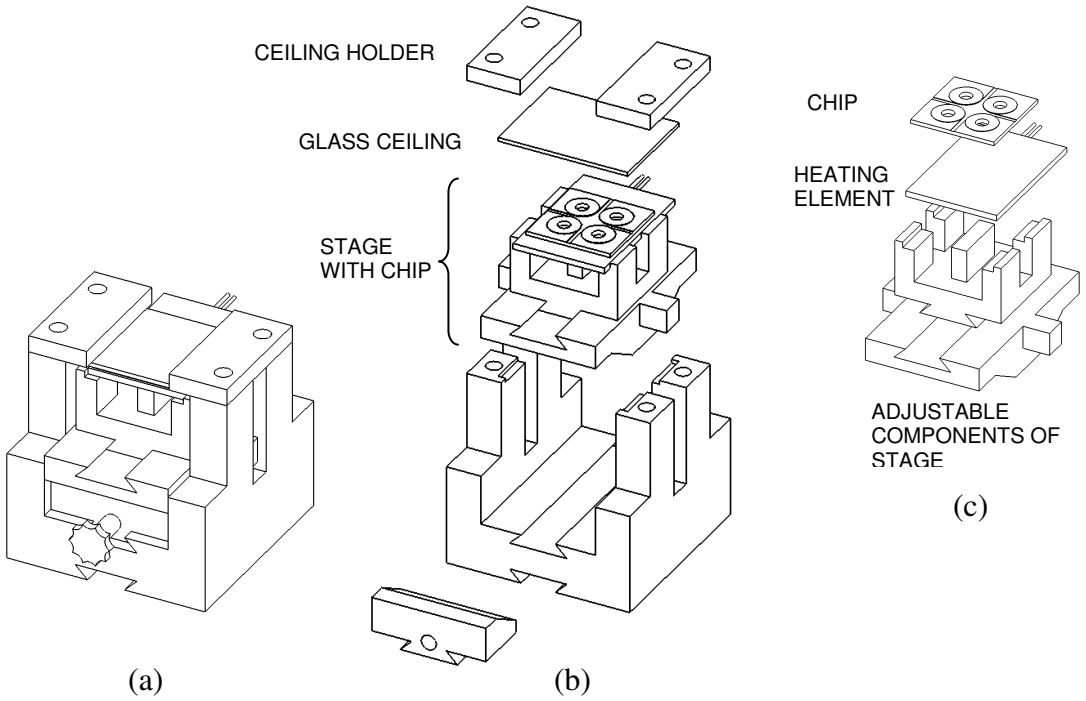


**Figure 10**. The first generation thermal cycler (a) assembled and (b) exploded. The third drawing (c) shows further explosion of the stage components.

unload the chip without disassembling components. By utilizing what are commonly referred to as dovetail tracks, the components were able to slide in specific directions. Together, the pieces that are able to be raised and lowered (to apply and remove pressure) are referred to as the stage. When the stage is lowered, the upper portion of the stage (holding the chip) is able to slide in and out of the central area. This provides simple access to samples. Glass was used for the ceiling of the thermal cycler. Although the material was fragile, transparency was necessary for the fluorescent detection system which viewed the sample wells from above (as heating took place from below).

## Chip Fabrication

As previously stated, soft lithography was used to produce the pattern on one side of the PDMS chip. In the process, a converse of the desired pattern in photoresist is

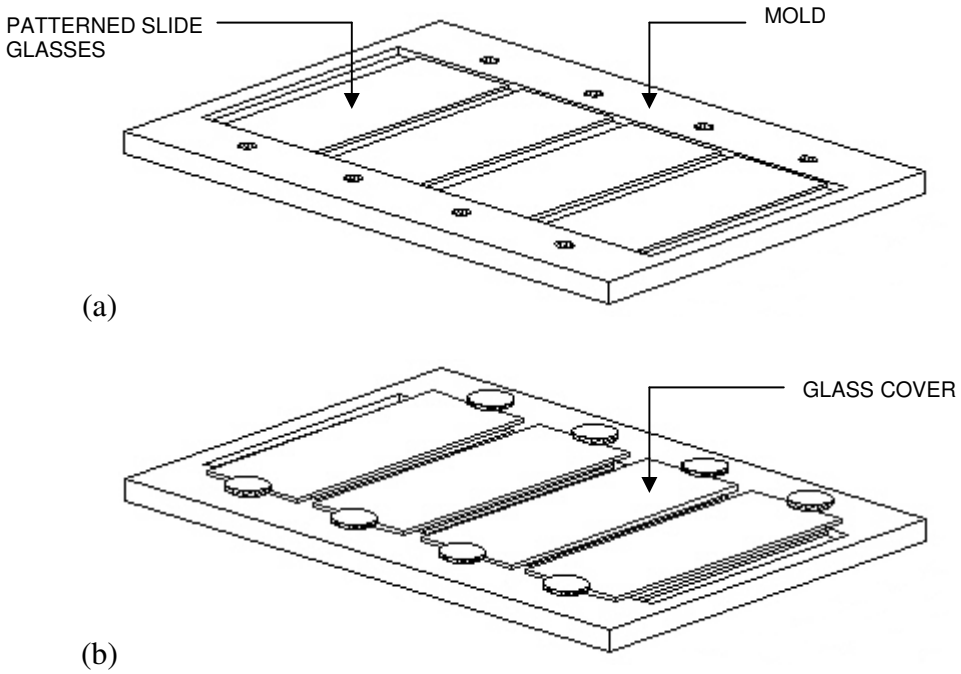


**Figure 11**. The first generation mold used to fabricate multiple chips simultaneously (a) without the longer glass cover and (b) with the longer glass cover fastened in place.

created using photolithography with a slide glass for a substrate. PDMS is then poured over the pattern and cured such that it takes on the desired pattern. To reduce this fabrication time (which is of utmost important for disposable chips), a mold was used that allowed for the fabrication of eight chips simultaneously. This original mold (referred to as the first generation mold), seen in Figure 11, securely held four slide glasses that had been previously patterned with photoresist. PDMS was poured onto each of the slide glasses to evenly coat the surface. A longer piece of glass was then placed over the patterned slide glass "sandwiching" the PDMS. This longer glass cover was held a specific distance from the patterned slide glass by the edge of the mold so that the PDMS would cure to the correct thickness. Once in place, the longer glass cover was fastened to the mold. Excess PDMS would flow from the patterned slide glass to overflow grooves within the mold. Once cured, the PDMS was removed from the mold and trimmed. The

circular lids were fabricated by pouring uncured PDMS into an area on a slide glass bound by an adhesive of desired thickness. A smooth film was then placed over the slide glass to ensure a smooth and transparent surface when finished. Under pressure, the PDMS was cured on a heating plate to create a thin film of PDMS. A punch was then used to cut the circular lids from this film.

## Failure Due to Bubble Formation

One of the more problematic issues while utilizing the polymerase chain reaction is the formation of bubbles. When performing *real-time* PCR, this problem further complicates the process as optical clarity is required. It should also be noted that if one is performing real-time PCR for reaction volumes at or below 10 μl, these effects are amplified. There are many causes to bubble formation such as the porosity of PDMS, poor sample loading, or inadequate bonding between PDMS and its substrate (in this case a glass cover slip). During sample loading, micropipettes are used to inject the sample into the reaction wells of the chip. As the sample is dropped into the well, it is possible for micro-bubbles to form in the imperfections of the walls of the well. These cracks and blemishes are common in pieces fabricated by means of soft lithography, but most can be attributed to the punch used to cut the circular well from the chip. When the sample is heated during thermal cycling, these bubbles expand and break the seal found between the reaction chamber and the substrate. Even if the bubble does not grow to be large enough to purge the sample from the well, its optical characteristics nullify real-time optical data collected.

One solution to bubble formation is to pressurize the sample. As previously discussed, this is why the thermal cycler included a stage (upon which the loaded chip was placed) that could be raised and lowered toward an optically clear ceiling of glass. The PDMS chip and lid would compress and pressurize the sample. Naturally, this created a second problem: the glass ceiling would reach its mechanical limits and break. During the initial compression, the lid would press firmly onto the chip and dispense overflow sample into the draining channels. The glass ceiling was able to withstand this initial pressure, it was during further denaturing steps that the glass would reach its limits as the compressed PDMS would undergo thermal expansion. Following these observations it was realized that there was a fine balance between applying enough pressure to prevent bubble formation and not overworking the 1 mm thick glass ceiling.

### Failure Due to Ceiling

Several steps were taken to correct this issue. First, it was believed that the inconsistency in circular lid thickness further perpetuated the problem. If lids of different thicknesses were used, it would take more compression for one lid over another, resulting in a stronger force on the glass from the thicker lid. To quickly resolve this problem, thicker lids were implemented. The effects of lid inconsistency were reduced due to size of the tolerance with respect to the overall thickness of the lid. This quick fix helped reduce the formation of bubbles, but as the loaded chip underwent thermal cycling, the glass ceiling would still crack occasionally. The next effort to fix this problem was the use of a different style ceiling holder. Prior to this point, the glass ceiling had been

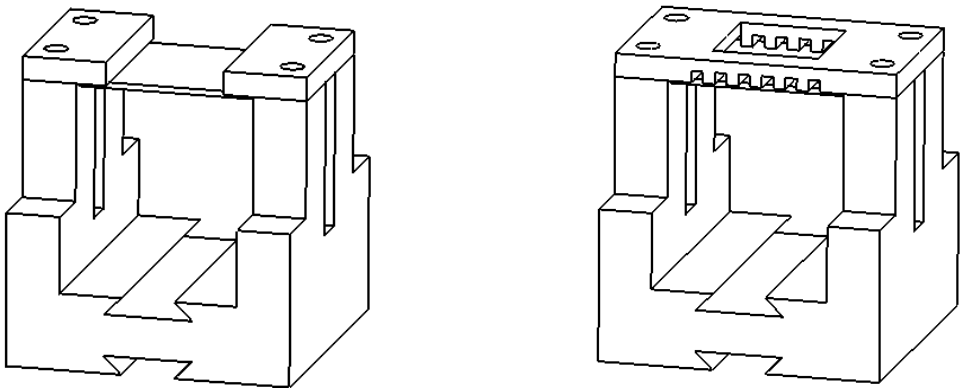


**Figure 12**. (a) The original glass ceiling holder securing the ceiling only at its edges and (b) the new holder bracing the ceiling at every edge.

secured at two of its edges. During compression, the chip would exert a force in the center of the glass ceiling causing the glass to bow at the unsupported edge. To further brace these free edges, the new ceiling holder, pictured in Figure 12, consisted of one piece stretching the length of the glass ceiling with an area removed for viewing from above. Although this reduced the flow of air supplied by the fan during the cooling process, it was necessary to reduce possibility of breaking the glass. Although these corrections succeeded in reducing the frequency of failure, it was decided at this point that a more permanent solution was necessary if such technology were to be realized in the market. This decision led to the design of a second generation mold for fabrication, a new fabrication procedure to smoothen the walls of the reaction chamber, and vast improvements of the thermal cycler.

New Chip Fabrication Method

The original mold described previously (see Figure 11) used slide glasses patterned with photoresist to form structures desired. Uncured PDMS was poured over these patterns and cured beneath another slide glass secured at each end. There were two characteristics under focus in the design of the second generation mold: overall improvement of the draining channels and consistency in both chip and lid thickness. PCR chips used in these studies were 1 mm in thickness. To prevent the risk of well-to-well contamination, the draining channels were widened and deepened. This allowed for the sample dispensed during compression to flow more freely from the reaction chamber into the larger-volume draining channels. The distance between each reaction chamber greater and the draining channels now deeper, thus reducing the possibility of sample migrating from one well to another. To improve in the consistency of lid thickness, several features of the original mold were altered. It was decided that more pressure was

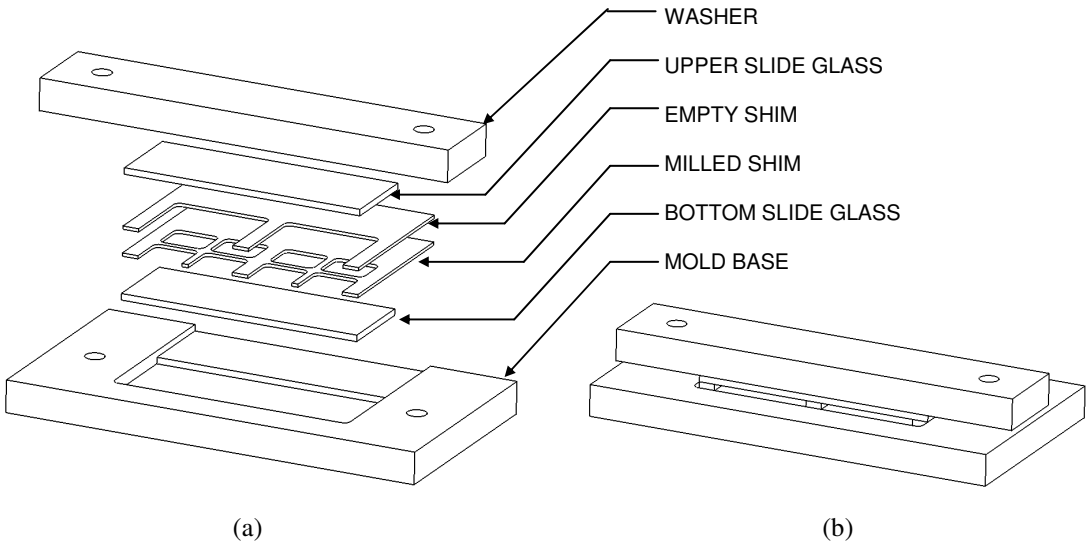


**Figure 13**. The second generation mold in both the (a) unloaded and (b) loaded positions.

required to ensure the desired thickness. To accomplish this, durable, metallic molds were fabricated with thick washers extending the length of the mold to apply pressure. Figure 13 depicts the new mold in both the unloaded and loaded positions.

The base of the mold contained a deep area slightly larger than the size of a standard slide glass. To use the mold, a slide glass was placed within this area. Two brass shims were then placed over this slide glass. Uncured PDMS was poured into the area formed from these shims and a second slide glass was then placed directly above these shims. Finally, the thick, rectangular washer was positioned over these objects, "sandwiching" them together. This washer was bolted down at each end until the pieces were held securely together. Each part served a specific purpose. The slide glasses at the top and bottom served to create a smooth, transparent surface for the PDMS chip that would not be possible if the PDMS were in direct contact with the mold base and washer. The two brass shims between the slide glasses were essential in forming a chip of the desired thickness. Each shim was 0.5 mm in thickness, thus creating a 1 mm thickness chip when used together. The bottom shim had been milled such that when the uncured PDMS was poured, it would fill the regions milled out to form the desired shape of the chip. The upper shim had also been milled to take on an "empty" form. This was necessary so that the chip was 1 mm in overall thickness while forming the 0.5 mm deep draining channels. After the upper slide glass was positioned over the area holding the liquid phase PDMS, the washer was then bolted over the collective pieces. This purged the air from the PDMS within the region between the slide glasses. The deepest area of the mold holding the lower slide glass designed to leave room for overflow PDMS. In

order to form the lid used with the chips during PCR, the same mold was used, but with a single shim of 1 mm thickness. Figure 14 depicts this setup. The mold is loaded in a similar manner, but the PDMS is cured free of the milled features that create the draining channels. A single lid replaced the individual circular lids used over each well from this point forward to simplify the chip loading process. The end result was a chip and lid of consistent thickness fabricated without the use of photoresist. This chip can be seen in Figure 15.

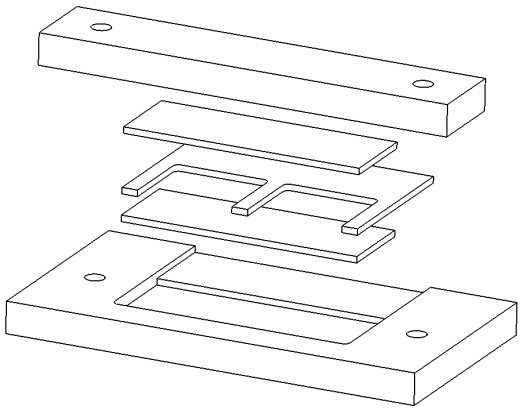

**Figure 14**. The second generation mold utilizing a single 1 mm shim to form the single square lid used with the chip during PCR.

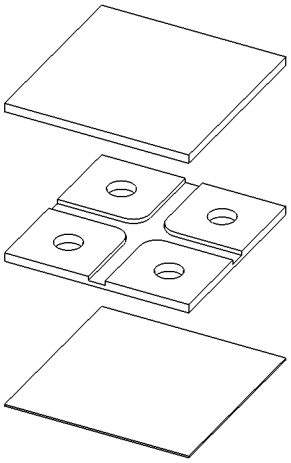

**Figure 15**. Schematic of a PCR chip and lid formed with the new molds (after the reaction wells have been punched) with its slide glass substrate.

## Alteration to Micro-well

The new chips were simple to manufacture and provided more consistent results. This new design yielded fewer failures due to glass cracks and much better sealing between the reaction chamber and the lid. However, at times, it was noticed that bubbles would occasionally form in the reaction chamber. Upon closer inspection, it became clear that the bubbles were forming between the chip and substrate. Prior to this point, the substrate and chip were bonded by bringing the corresponding surfaces together after plasma treatment. To both, improve the seal between the chip and substrate and eliminate imperfections in the walls of the reaction well, a new procedure was added to the fabrication process. The technique, realized by Liu et al. [30], utilized additional PDMS and a second curing procedure to smooth the walls. In this process, a portion of the uncured PDMS mixture was poured onto the cover slip substrate, degassed, and spun on a spin-coater to the desired thickness. The previously cured chip was then placed onto the substrate holding the uncured PDMS. This allowed for the liquid PDMS to flow into the imperfections found on the well wall. As the PDMS settled, it also formed a curved surface between the well wall and the substrate, creating a bowl-shaped base to the reaction well. The composition was then cured a second time, allowing the uncured PDMS to bond with the cured PDMS structure. These characteristics are further depicted in Figure 16. This extra step in fabrication prevented the occurrence of bubbles forming at the bottom of the well due to a poor seal or blemishes in the PDMS. It also formed a stronger seal between the chip and substrate.

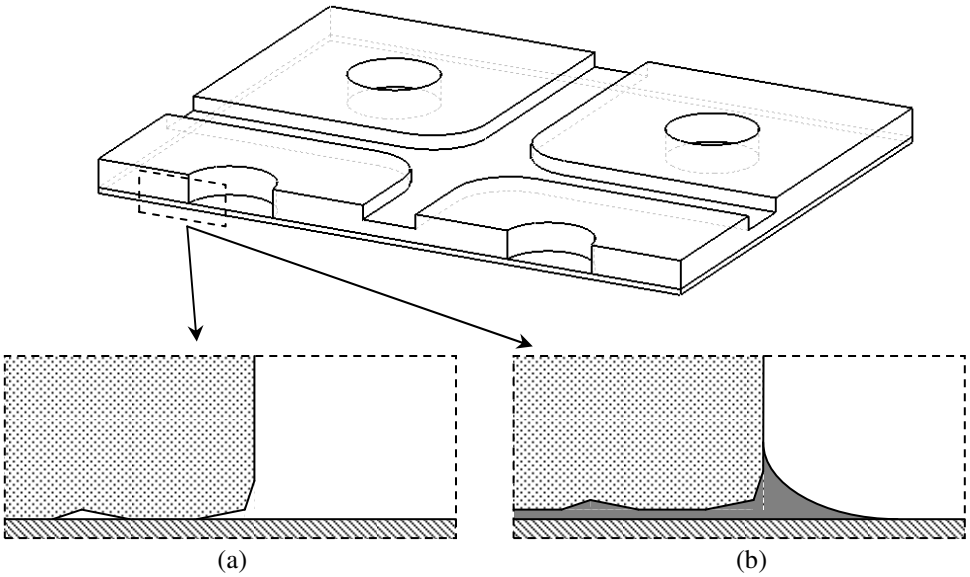


**Figure 16**. Schematic of a PCR chip (a) before and (b) after implementing the new technique involving the addition of PDMS and second curing procedure.

## Fog Formation

With these improvements, repeatability was raised significantly. While using the single square lid, however, a new issue became prevalent. It could be observed that as the thermal cycling began, a fog would appear within the center of the well and even in the edges of the well. Upon further inspection under the microscope, the conclusion was made that the natural porosity of PDMS was allowing bubbles to grow within the structure of the chip and the square lid. This is not an uncommon problem when using PDMS for this application, thus various researchers have found novel methods of prohibiting the migration of fluid through the material. One such technique is applying an impermeable coat of Parylene to the PDMS [31]. To avoid additional costs in fabrication of the chip, the similar yet simple solution of adding a thin plastic film to the square lid was implemented. This optically clear film was trimmed to the dimensions of the 1 mm

PDMS lid and fastened to the side in direct contact with the sample. Results were as expected; the fogginess subsided.

## Thermal Cycler Redesign

Other than the layout of the microfluidic chip itself, the most important section of a microfluidic PCR system is the thermal cycler. As described previously, the thermal cycler in this study utilized a knob that, when turned, would raise and lower the chip. This allowed the chip to be easily loaded and unloaded from the stage. Delrin was milled with a CNC system to fabricate the first generation unit. This unit, pictured in Figure 17(a), incorporated pathways above and below the compressed chip and ceiling to allow for more airflow to cool the chip faster while the blower-style fan was in use. Design of the second generation unit, pictured in Figure 17(b), focused on compression of the chip and ceiling. A piece of quartz replaced the 2 mm thick slide glass ceiling to eliminate the possibility of cracking. A new safety feature was also incorporated to prevent the user from applying too little or too much pressure. The quartz holder was designed with a physical stop on it such that the stage could not be raised past a specified height. This height could be adjusted by adding or removing thin plates (fashioned shims). A rapid prototyper was used to fabricate this second generation thermal cycler. The ease and low cost of this additive manufacturing process allowed for further improvements of the system, yielding a third generation thermal cycler (see Figure 17(c)). Made similarly, with ABS plastic, the third generation thermal cycler was focused on size and functionality. This final design was smaller in size when compared to the first generation

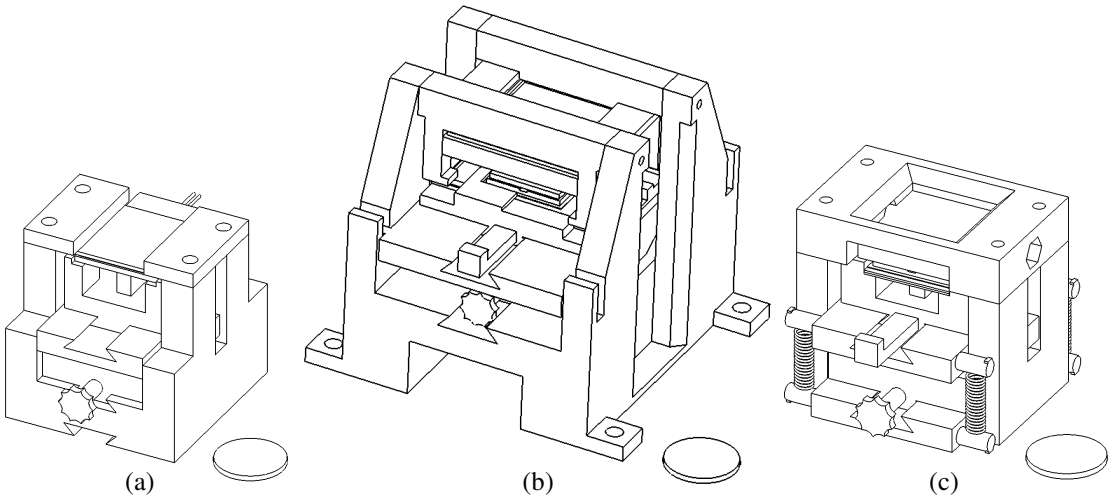


**Figure 17**. The (a) first generation, (b) second generation, and (c) third generation thermal cyclers pictured with a penny next to each for a size perspective.

.

system while implementing similar characteristics experimented with in the larger second generation. Springs were added to prevent sticking of the chip to the ceiling. The quartz ceiling was fastened to a separate upper piece and the stage included an alignment element to ensure that the chip was properly aligned during every test. Airflow passageways were widened and the stage was formed from a heating element compressed between two thin shims coated in thermal paste. Through a series of redesigns the thermal cycler evolved into a user-friendly system capable of obtaining consistent results without sacrificing size.

# CHAPTER IV

# METHODOLOGY

The PCR chips are comprised of three layers: a substrate, a molded pattern of wells, and a lid. A substrate provides rigidity while serving as the bottom to the well. Reaction wells hold the samples in close proximity while draining channels preventing cross contamination. This structure is bonded to the substrate with PDMS by means of a second curing procedure. Once the wells are loaded, the lid is placed over the chip and compressed to ensure proper sealing.

## PCR Chip Fabrication

Liquid Sylgard 184 base (Dow Corning, Midland, MI) and its curing agent were thoroughly mixed in a weight ratio of 10:1. To cast the draining channels, the mixture was poured into a mold that ensured an overall thickness of 1 mm and a draining channel depth of 0.5 mm. After degassing for one hour, the PDMS was cured at 75 ºC for three hours. The solidified pattern was then removed and trimmed to the size of the substrate: a 22 × 22 × 0.1 mm micro cover glass (VWR International, West Chester, PA). Wells with a diameter of 3.175 mm (1/8 inch) were then punched from the pattern. To bond the substrate and cast together, a second curing procedure was implemented. Uncured PDMS was spun onto the substrate, the previously-cured cast was then placed onto this substrate and the two pieces were cured a second time to form a smooth bottom surface for the reaction well.

A flexible PDMS lid formed in an equivalent manner as with the previous cast (but without the draining channels) was trimmed to the same dimensions as the substrate. To prevent fogging in areas of the lid near the well resulting from the permeability of PDMS, an optically-clear PCR film (Axygen Scientific, Union City, CA) was adhered to the lid so the sample was not in direct contact with it. The samples were then loaded into the wells in a volume (10 μl) greater than that of the well volume to ensure there was enough sample to overflow into the draining channels. This loading procedure was done to prevent air from being trapped in the well during compression. The flexible property of the PDMS was then taken advantage of by compressing the chip and lid together to pressurize the loaded sample to prevent bubble formation and evaporation. Refer to Figure 15 for an assembly of the PCR chip.

## Reagents

The primers were designed by Mason et al. in the study of a PCR protocol designed to diagnosis staphylococcal infection. The particular set used in this paper correspond to a 306 bp fragment of the 791 bp regions of the 16S rRNA genes shared solely among Staphylococci when compared to other eubacterial species [32]. The primer set (Gene Link, Hawthorne, NY) is: forward, 5′-CCT ATA AGA CTG GGA TAA CTT CGG G-3′, and reverse, 5′-TTT ACG ATC CGA AGA CCT TCA TCA-3′. The TaqMan probe was labeled with AlexaFluor 647 reporter dye and BHQ3 quencher dye with the following sequence: AlexaFluor 647 5′-GGA GCT AAT ACC GGA TAA TAT TTT GAA CCG CA-3′ BHQ3. The excitation and emission peak of

AlexaFluor 647 are 650 nm and 670 nm, respectively. All other reagents were purchased from Promega (Madison, WI). A 100 µl PCR mixture contained 65 µl of deionized water, 4 µl of each primer (25 µM each), 2 µl of probe (10 µM), 2 µl of dNTPs (10 mM each, 40mM in total), 20 µl of 5× Buffer, 1 µl of Taq (5 U/µl), and 2 µl of template. Each cycle was comprised of three stages: denaturation at 94ºC for 30 s, annealing at 54ºC for 60 s, and extension at 72ºC for 60 s. Each PCR run began with an initial 5 min denaturation at 94ºC.

## Sample Preparation

Clinical MRSA isolates were recovered from stock cultures maintained at –70 ºC. After inoculation on tryptic soy agar with 5% sheep blood (Hardy Diagnostics, Santa Clara, CA), isolates were confirmed to be *S. aureus* by coagulase testing via latex agglutination. Template DNA was prepared using three different methods. For boiled specimens, staphylococcal colonies were collected with a 1-µl loop and placed in sterile water. After vortexing, specimens were heated to 99 ºC for 15 minutes, then kept on ice until utilized in the real-time PCR reaction. For crude DNA preparation, staphylococcal colonies were collected with a 1-ul loop, placed in a 5% lysostaphin solution, incubated at 37 ºC for 15 minutes, and pelleted by centrifugation. After resuspension of the pellet in 100 µl sterile water, samples were boiled for 15 minutes. For purified genomic preparations, the UltraClean Microbial DNA Isolation Kit (Mo Bio Laboratories, Carlsbad, CA) was used per manufacturer's microbial-specific instructions.

## Miniature Thermal Cycler

The miniature thermal cycler described previously was used in controlling the temperature of the sample and to apply pressure to the PCR chip. To heat the sample, a thin heating element was placed between two thin aluminum shims and fastened onto the stage. Beneath this stage existed airways that run parallel to the direction of flow of air from a cooling fan. The heating power was adjusted according to temperature feedback control supplied by a thermocouple embedded between the aluminum shims. Data was collected with a data acquisition card (DAQPad-3020E, National Instruments Corp.). The system was designed such that the stage holding the chip and lid were raised toward an upper quartz surface. This quartz ceiling was used to compress the chip and lid together to ensure proper sealing of the sample well. It also served to pressurize the sample to reduce bubble formations and to improve contact between the chip substrate and the heated aluminum shim. The stage was fixed to tracks that allowed it to slide in and out of the quartz area for easy loading and dispensing. Because the thermocouple used for feedback control was not a direct measurement of the well temperature, the heating program had to be calibrated. To do so, a calibration chip was fabricated with a thermocouple embedded directly into the well and loaded with water. This setup was then used in the system to measure the difference in temperature profiles between the two thermocouples throughout the duration of a mock test and alter the heating power accordingly. Figure 18 visualizes the actual well temperature during a test ran with water as measured by the embedded thermocouple after calibration.

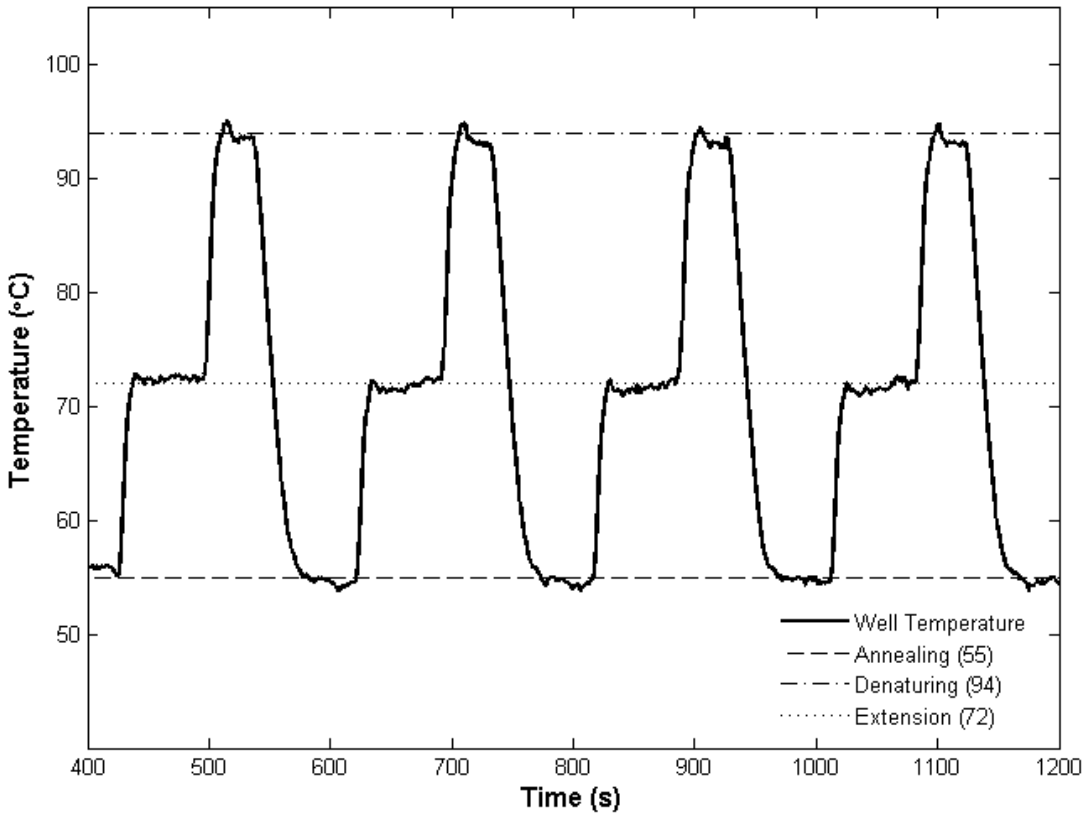


**Figure 18.** The actual temperature of the loaded reaction well during a PCR as measured by a thermocouple embedded within the chip with the end exposed inside the well. The PCR conditions include denaturation at 94ºC for 30 seconds, annealing at 55ºC for 60 seconds, and extension at 72ºC for 60 seconds.

One of the more prominent concerns with high-throughput well-based PCR, whether it is a macro or micro-scale system, is well-to-well temperature consistency. To validate that each well was being heated and cooled to the appropriate temperatures, the calibration chip was rotated to record the temperature of each well through a series of temperature cycles. Figure 19 plots the temperature recorded through one complete cycle with the desired temperature. Slight overshoot can be seen for each well with an approximate well-to-well deviation of ±1.5 ºC.

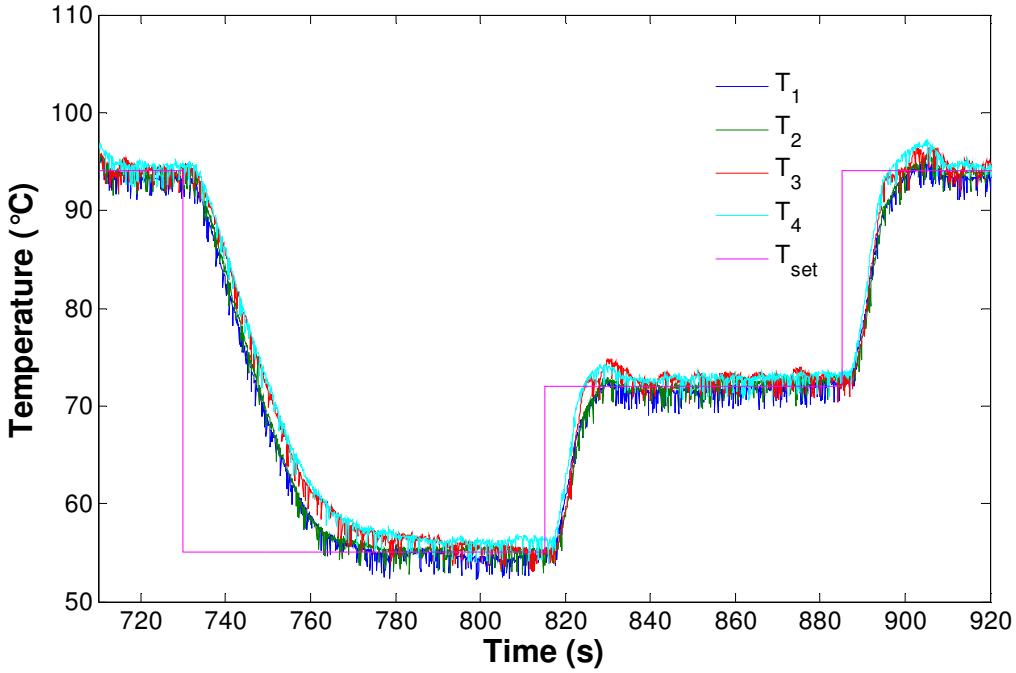


**Figure 19.** The recorded temperature of each well for a complete cycle with the desired temperature for the reaction to visualize well-to-well deviation.

## Fluorescent Detection

The miniature thermal cycler was used in conjunction with a fluorescent microscope (AZ100, Nikon Instruments Inc.) to record intensity measurements required for real-time PCR. A CCD camera (CoolSNAP ES, Photometrics) acquired measurements and data which were collected through the computer using image analysis software (NIS-Elements, Nikon Instruments Inc.). This software was capable of measuring the average fluorescent intensity of a specified region. Excitation light of 650 nm was supplied at intervals during the annealing stage and the average fluorescent intensity value (670 nm emission) was used to represent each cycle. The annealing stage was selected based on previous findings regarding the temperature dependence of the reporter dye [33].

# CHAPTER V

# RESULTS

## Sample Preparation Experimental Results

The experiments performed were based on a TaqMan real-time polymerase chain reaction with primers designed to produce amplicons of 306 bp size found within a region of the 16S rRNA genes unique to staphylococci with respect to other eubacterial genes. The template supplied was methicillin-resistant *Staphylococcus aureus*. Experiments were performed to verify the micro-PCR system's capacity to detect MRSA under three varying degrees of sample preparation. Secondly, a serial dilution test was used to investigate the system's efficiency.

In order to demonstrate the ability to amplify MRSA based on the three templates provided under differing DNA preparation methods, real-time PCR was conducted under the conditions stated previously for each. Figure 20 plots the mean fluorescent intensity at each cycle for each form of template. The desired fluorescent intensity curve is apparent for each form of template. During the early cycles of each curve, approximately prior to completion of the 15th cycle, the intensity value is minimal with little fluctuation. This is followed by dramatic increase in measured fluorescent intensity for the next 15-20 cycles which gradually tapers to what is commonly referred to as the plateau stage. This result follows the fluorescence resonance energy transfer (FRET) fundamentals of TaqMan probe-based PCR as the reporter dye is only able to emit light once it is cleaved from the

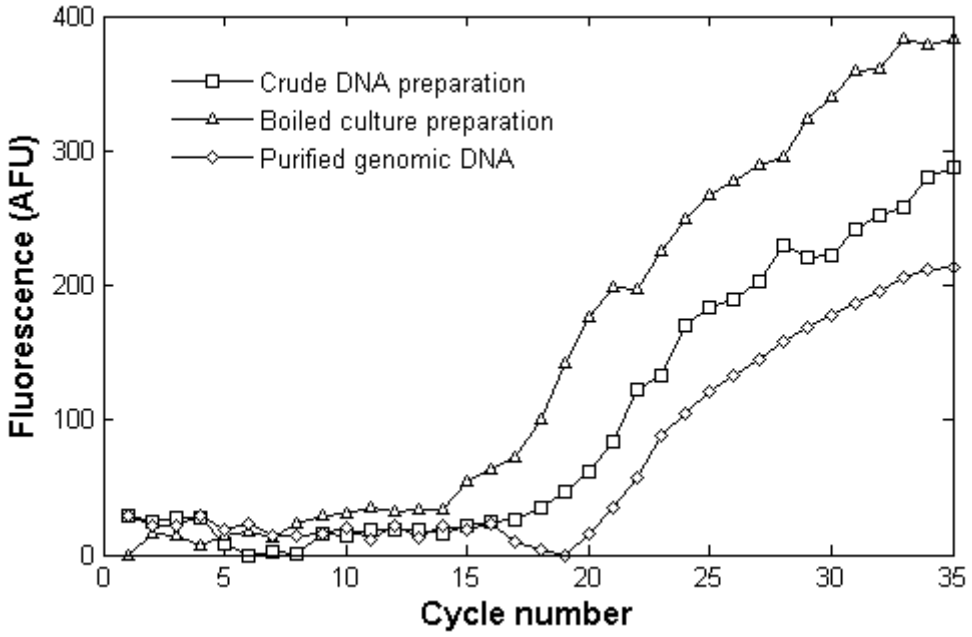


**Figure 20.** Measured mean fluorescent intensity at each cycle of the PCR for each form of template. Each curve follows the common trend seen in TaqMan probe-based PCR.

quencher dye following reproduction of the desired DNA fragment. The resulting increase in light is proportional to the amount of amplicons produced in that cycle. During the initial stages of the reaction, the increase in light, and thus, the increase in amplicons, went undetected by the optical system due to the low initial concentration. Once the number of fragments produced was great enough, the overall fluorescent intensity emitted from the reporter dye passed the detectable threshold and a curve formed as the plot entered the exponential phase. Finally, as reagent consumption limited the reaction, a plateau in measured intensity could be seen.

## Verification

To verify the results, the same samples were ran on a commercial thermal cycler (Mastercycler, Eppendorf). A gel electrophoresis was then performed on the products of both the commercial thermal cycler and the micro-PCR system. The expected 306 bp size is verified in the results depicted in Figure 21. The first lane in the image is a ladder with markers at intervals of 100 bp beginning with 100 bp. The subsequent eight lanes (2-9) are the results of the commercial thermal cycler with duplicates of each form of template. The second and third lanes contain boiled culture preparation template, the fourth and fifth lanes contain purified genomic DNA template, the sixth and seventh lanes contain crude DNA preparation template, and the eighth and ninth lanes are negative control (master mix with no template). The following three lanes (10-12) are from the boiled culture preparation template run on the micro-PCR system with lane 12 holding the negative control. The next three lanes (13-15) contain the gel electrophoresis results for the purified genomic DNA template run on the micro-PCR system with lane 14 holding the negative control. Held in the final three lanes (16-18) are the crude DNA preparation results of with the negative control in lane 16. A 10 µl

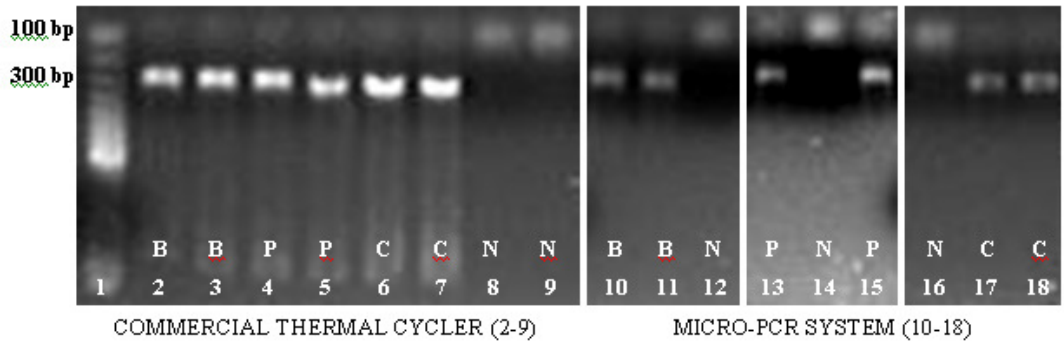


**Figure 21.** Gel electrophoresis results from both the commercial thermal cycler and the designed micro-PCR system for each form of template. The bands seen correspond to the 300 bp marker on the ladder in the first lane. Lanes labelled with B represent boiled culture preparation, P represent purified genomic preparation, C represent crude preparation and N represent negative control (master mix without template).

sample size was used in the commercial thermal cycler and thus 10 µl was available for use in the gel electrophoresis after the test with these samples (lanes 2-9). Although 10 µl of sample is dispensed into the reaction well of the microfluidic chip for the designed micro-PCR system, the reaction well itself could not hold 10 µl per design. This allowed for overflow of the sample into the draining channels to ensure proper sealing and reduce bubble formation. Because of this, and due to the difficulty in retrieving completed samples from the microfluidic chip, it was only possible to extract approximately 6 µl of the finished sample from the reaction well for gel electrophoresis. This can account for the reduced fluorescent intensity of the resultant band of the samples ran on the micro-PCR system (lanes 10-18) in comparison to those ran on the commercial thermal cycler. Regardless of intensity, for each case containing template, a band of PCR product corresponding to the 300 bp marker on the ladder is seen. The gel results verify that amplification of the correct size PCR product was achieved.

## Serial Dilution and Standard Curve

A 10-fold serial dilution of purified genomic DNA template was prepared with concentrations ranging from 93.1 to 0.0931 ng/µl. Real-time PCR was conducted in each of the concentrations and the amplification plots of each can be seen in Figure 22. A standard curve was generated from these results and is shown in Figure 23.

For this portion of testing, the lowest concentration that provided clear amplification from the system was 0.0931 ng/µl. Based on the 10 µl sample size

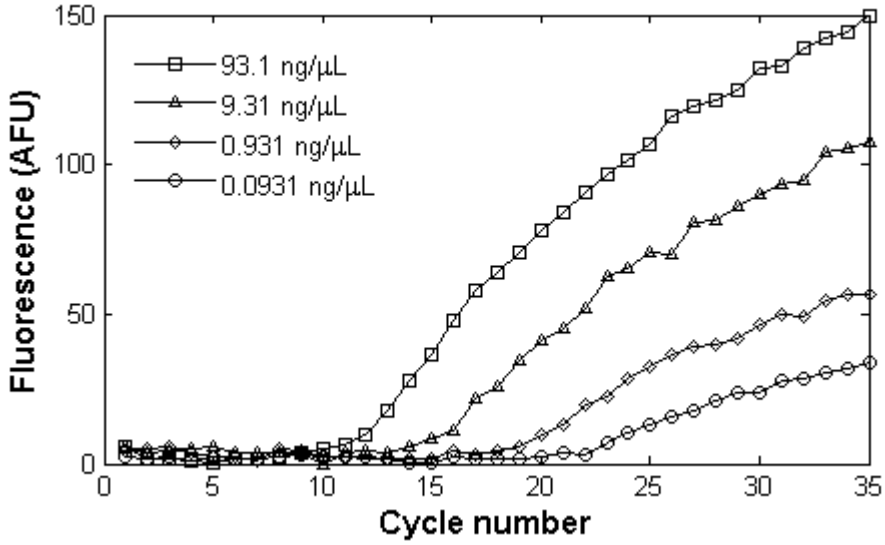


**Figure 22.** Mean fluorescent intensity at each cycle for four concentrations of a 10-fold serial dilution test of purified genomic MRSA DNA.

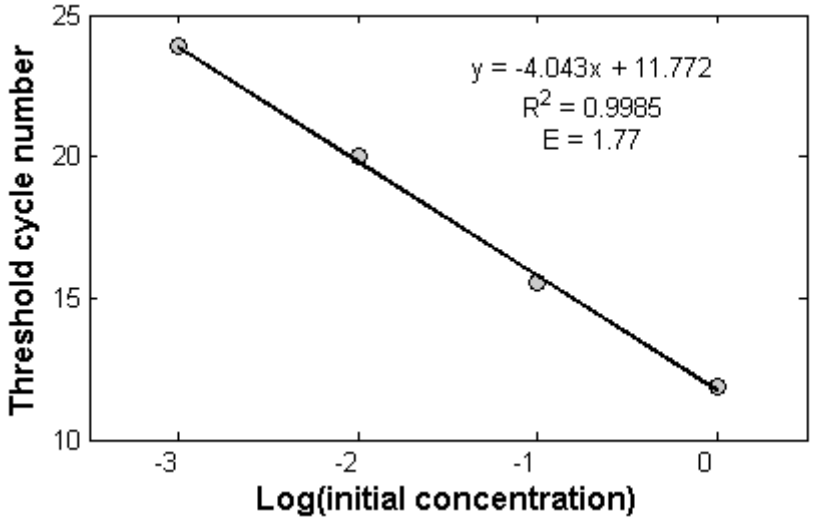


**Figure 23.** Standard curve of the micro-PCR system based on a 10-fold serial dilution from 100% (93.1 ng/µl) to 0.1% (0.0931 ng/µl). The amplification efficiency calculated based on this curve is 1.77.

injected into each well and a ratio of 2 µl of template in a 100 µl sample mixture, a 10 µl sample with 18.6 pg of DNA provided clear amplification. Based on a 2.8 Mb

genome length, that equates to roughly 12,000 copies in a 10 µl sample. A standard curve was generated with these results and is shown in Figure 6. The amplification efficiency calculated based on this standard curve is 1.77 out of a theoretical 2.0 indicating a doubling of DNA per cycle.

## Sample Volume Reduction

In an effort to help quantify the capabilities of the system, new chips were designed to run the same assay with purified genomic DNA at a smaller volume. These chips were of a similar design as previously used, however, the well diameter was reduced to create a smaller micro-reaction chamber with a larger aspect ratio. The concentration was reduced until clear amplification could be seen consistently. Under these conditions, a 3 µl reaction volume (the smallest tested) containing 11.2 pg of DNA provided clear positive results with an approximate threshold cycle of 20 cycles.

The scope of this work did not include optimization of the PCR protocol and micro-PCR system. The purpose was to investigate the feasibility of using this micro-PCR system for MRSA detection under minimal sample preparation. Based on this, it is believed that the reaction time can be reduced and amplification efficiency improved.

# CHAPTER VI

## CONCLUSIONS AND FUTURE WORK

It was experimentally demonstrated in this work that the developed micro-PCR system is capable of successfully amplifying methicillin-resistant *Staphylococcus aureus* DNA based on three degrees of sample preparation: purified genomic DNA, crude DNA preparation and boiled culture preparation without any additional reagents. A four-well stationary, microfluidic PCR chip fabricated with only PDMS, a glass cover slip, and a thin plastic film reduced fabricating costs in comparison to more expensive silicon chips. Such a platform for disposable chip design could prove essential to reducing costs associated with proposed portable PCR systems. A sample size of 3 μl containing only 11.2 pg of purified genomic DNA was successfully amplified. The system developed in this work is capable of detecting MRSA prepared through simple boiled culture without the use of any additional reagents. This is a significant step in the development of a point-of-care detection system capable of identifying microorganisms such as MRSA with little or no pre-PCR manipulations.

It has been verified that the current system is capable of detecting MRSA with little or no preassay manipulations. However, the system must be utilized for clinical trials before conclusions can be drawn. The ultimate goal is to detect staphylococcal DNA from purulent fluid or infected joint fluid at a patient's bedside.

Much work is still needed to optimize the performance of the system. Current assay times can be over two hours long, comparable to most commercial systems. One of the advantages of using such small sample sizes is the potential to reduce assay time as it takes less time to heat and cool the bioreactor and sample. This has not yet been taken advantage of within this work in an effort to eliminate possible sources of inefficiency. Further studies on temperature holding time should reduce this testing time dramatically. The design of the miniature thermal cycler used in this study is flexible with respect to improvements of the throughput of the system. Much of the tests completed in this study were performed at 10 µl sample size, however, a 3 µl sample size was also succesfully verified. Through this, it is possible to manufacture a microfluidic chip of the same size with smaller and more numerous bioreactors. A 3 x 3 or perhaps a 4 x 4 micro-well chip would greatly improve the capabilities of such a device. Possible hindrances to such expansion are the draining channel width and well to well temperature uniformity.

With regards to temperature, it is also possible to improve both the assay time and temperature uniformity through minor design alterations to the thermal cycler. A study should be performed on the material with which the system was manufactured. ABS plastic and Delrin were used simply due to their ease of manufacturing, however, it may be possible to enhance heat transfer during both the cooling and heating stages by incorporating different materials in the device. Lastly, the capabilities of the described system would be expanded through the use of multiple light filters for multiplex polymerase chain reaction. Although this is not possible

with the current setup, alteration of the optical detection system to incorporate a selection of filters would enable for multiple independent assays to be conducted at the same time. This, in combination with a high-throughput microfluidic chip, can vastly increases the potential of this system.

# REFERENCES


1 M. A. Northrup, M. T. Ching, R. M. White and R. T. Watson, *In Transducers '93, the 7th International Conference on Solid-State Sensors and Actuators*, Yokohoma, Japan, 1993, 924-6.

2 Q. Xiang, B. Xu and D. Li, *Biomedical Microdevices*, 2007, 9, 443-49.

3 P. Belgrader, S. Young, Bob Yuan, M. Primeau, L. A. Christel, F. Pourahmadi and M. A. Northrup, *Analytical Chemistry*, 2001, 73, 286-9.

4 J. A. Higgins, S. Nasarabadi, J. S. Karns, D. R. Shelton, M. Cooper, A. Gbakima and R. P. Koopman, *Biosensors and Bioelectronics*, 2003, 18, 1115-23.

5 M. Hashimoto, P. Chen, M. W. Mitchell, D. E. Nikitopoulos, S. A. Soper and M. C. Murphy, *Lab on a Chip*, 2004, 4, 638-45.

6 E. T. Lagally, I. Medintz and R. A. Mathies, *Analytical Chemistry*, 2001, 73, 565-570.

7 D. Lee, S. H. Park, H. Yang, K. Chung, T. H. Yoon, S. Kim, K. Kim and Y. T. Kim, *Lab on a Chip*, 2004, 4, 401-7.

8 P. Wilding, M. A. Shoffner and L. J. Kricka, *Clinical Chemistry*, 1994, 40, 1815-8.

9 Y. Liu, C. B. Rauch, R. L. Stevens, R. Lenigk, J. Yang, D. B. Rhine and P. Grodzinski, *Analytical Chemistry*, 2002, 74, 3063-70.

10 J. Yang, Y. Liu, C. B. Rauch, R. L. Stevens, R. H. Liu, R. Lenigk and P. Grodzinski, *Lab on a Chip*, 2002, 2, 179-87.

11 B. C. Giordano, J. Ferrance, S. Swedberg, A. F. R. Hühmer and J. P. Landers, *Analytical Biochemistry*, 2001, 291, 124-32.

12 A. F. R. Hühmer and J. P. Landers, *Analytical Chemistry*, 2000, 72, 5507-12.

13 R. P. Oda, M. A. Strausbauch, A. F. R. Huhmer, N. Borson, S. R. Jurrens, J. Craighead, P. J. Wettstein, B. Eckloff, B. Kline and J. P. Landers, *Analytical Chemistry*, 1998, 70, 4361-68.

14 C. Ke, H. Berney, A. Mathewson and M. M. Sheehan, Sensors and Actuators B, 2004, 102, 308-314.

15 Y. Tanaka, M. N. Slyadnev, A. Hibara, M. Tokeshi and T. Kitamori, *Journal of Chromatography A*, 2000, 894, 45-51.

16 M. N. Slyadnev, Y. Tanaka, M. Tokeshi and T. Kitamori, *Analytical Chemistry*, 2001, 73, 4037-44.

17 S. A. Soper, S. M. Ford, Y. Xu, S. Qi, S. McWhorter, S. Lassiter, D. Patterson and R. C. Bruch, *Journal of Chromatography A*, 1999, 853, 107-20.

18 P. Gascoyne, J. Satayavivad and M. Ruchirawat, *Acta Tropica*, 2004, 89, 357-69.

19 M. U. Kopp, A. J. de Mello and A. Manz, *Science*, 1998, 280, 1046-8.

20 J. Liu, M. Enzelberger and S. Quake, *Electrophoresis*, 2002, 23, 1531-36.

21 M. Krishnan, V. M. Ugaz and M. A. Burns, *Science*, 2002, 298, 793.

22 E. K. Wheeler, W. Benett, P. Stratton, J. Richards, A. Chen, A. Christian, K. D. Ness, J. Ortega, L. G. Li, T. H. Weisgraber, K. Goodson and F. Milanovich, *Analytical Chemistry*, 2004, 76, 4011-6.

23 P. J. Obeid, T. K. Christopoulos, H. J. Crabtree and C. J. Backhouse, *Analytical C hemistry*, 2003, 75, 288-95.

24 G. Hu, Q. Xiang, R. Fu, B. Xu, R. Venditti and D. Li, *Analytica Chemica Acta*, 2006, 557, 146-51.

25 From the Center for Disease Control and Prevention, Four Pediatric Deaths From Community-Acquired Methicillin-Resistant *Staphylococcus aureus*-Minnesota and North Dakota, 1997-1999, *Morbid Mortal Weekly Report*, 1999, 48, 707-10.

26 S. K. Fridkin, J. C. Hageman, M. Morrison, L. T. Sanza, K. Como-Sabetti, J. A. Jernigan, K. Harriman, L. H. Harrison, R. Lynfield and M. M. Farley, *New England Journal of Medicine*, 2005, 352, 1436-44.

27 G. Martinez-Aguilar, A. Avalos-Mishaan, K. Hulten, W. Hammerman, E. Mason and S. L. Kaplan, *Pediatric Infectious Disease Journal*, 2004, 23, 701-6.

28 R. M. Klevens, M. A. Morrison , J. Nadle, S. Petit, K. Gershman, S. Ray, L. H. Harrison, R. Lynfield, G. Dumyati, J. M. Townes, A. S. Craig, E. R. Zell, G. E. Fosheim, L. K. McDougal, R. B. Carey and S. K. Fridkin, *Journal of the American Medical Association*, 2007, 298, 1763-71.

29 T. S. Naimi, K. H. LeDell, K. Como-Sabetti, S. M. Borchardt, D. J. Boxrud, J. Etienne, S. K. Johnson, F. Vandenesch, S. Fridkin, C. O'Boyle, R. N. Danila and R. Lynfield, *Journal of the American Medical Association,* 2003, 290, 2976-84.

30 H. Liu, H. Gong, N. Ramalingam, Y. Jiang, C. Dai and K. M. Hui, *Journal of Micromechanics and Microengineering*, 2007, 17, 2055-64.

31 Y. S. Shin, K. Cho, S. H. Lim, S. Chung, S. J. Park, C. Chung, D. C. Han and J. K. Chang, *Journal of Micromechanics and Microengineering*, 2003, 13, 768-774.

32 W. J. Mason, J. S. Blevins, K. Beenken, N. Wibowo, N. Ojha and M. S. Smeltzer, *Journal of Clinical Microbiology*, 2001, 39, 3332-8.

33 Q. Xiang, B. Xu, R. Fu and D. Li, *Biomedical Microdevices*, 2005, 7, 273-9.